NRC·CNRC

NRC Publications Archive
Archives des publications du CNRC

An observational perspective of low-mass dense cores I: internal physical and chemical properties

Di Francesco, James; Evans II, Neal J.; Caselli, P. (Paola); Myers, Phillip C.; Shirley, Yancy; Aikawa, Yuri; Tafalla, M. (Mario)

Publisher's version / Version de l'éditeur:

Protostars and Planets V, pp. 17-32, 2007

NRC Publications Archive Record / Notice des Archives des publications du CNRC :
https://nrc-publications.canada.ca/eng/view/object/?id=dd9cfecf-2e1e-4d8c-92b3-b29815d5e3d2
https://publications-cnrc.canada.ca/fra/voir/objet/?id=dd9cfecf-2e1e-4d8c-92b3-b29815d5e3d2

Access and use of this website and the material on it are subject to the Terms and Conditions set forth at
https://nrc-publications.canada.ca/eng/copyright
READ THESE TERMS AND CONDITIONS CAREFULLY BEFORE USING THIS WEBSITE.

L'accès à ce site Web et l'utilisation de son contenu sont assujettis aux conditions présentées dans le site
https://publications-cnrc.canada.ca/fra/droits
LISEZ CES CONDITIONS ATTENTIVEMENT AVANT D'UTILISER CE SITE WEB.

Questions? Contact the NRC Publications Archive team at PublicationsArchive-ArchivesPublications@nrc-cnrc.gc.ca. If you wish to email the authors directly, please see the first page of the publication for their contact information.

Vous avez des questions? Nous pouvons vous aider. Pour communiquer directement avec un auteur, consultez la première page de la revue dans laquelle son article a été publié afin de trouver ses coordonnées. Si vous n'arrivez pas à les repérer, communiquez avec nous à PublicationsArchive-ArchivesPublications@nrc-cnrc.gc.ca.

National Research Council Canada | Conseil national de recherches Canada

Canada

An Observational Perspective of Low-Mass Dense Cores I: Internal Physical and Chemical Properties

James Di Francesco
National Research Council of Canada

Neal J. Evans II
The University of Texas at Austin

Paola Caselli
Arcetri Observatory

Philip C. Myers
Harvard-Smithsonian Center for Astrophysics

Yancy Shirley
University of Arizona

Yuri Aikawa
Kobe University

Mario Tafalla
National Astronomical Observatory of Spain

arXiv:astro-ph/0602379v1 17 Feb 2006

Low-mass dense cores represent the state of molecular gas associated with the earliest phases of low-mass star formation. Such cores are called "protostellar" or "starless," depending on whether they do or do not contain compact sources of luminosity. In this chapter, the first half of the review of low-mass dense cores, we describe the numerous inferences made about the nature of starless cores as a result of recent observations, since these reveal the initial conditions of star formation. We focus on the identification of isolated starless cores and their internal physical and chemical properties, including morphologies, densities, temperatures, kinematics, and molecular abundances. These objects display a wide range of properties since they are each at different points on evolutionary paths from ambient molecular cloud material to cold, contracting, and centrally concentrated configurations with significant molecular depletions and, in rare cases, enhancements.

1. INTRODUCTION AND SCOPE OF REVIEW

Over the last decade, dedicated observations have revealed much about the earliest phases of low-mass star formation, primarily through studies of low-mass dense cores with and without internal protostellar sources, e.g., protostellar and starless cores. Such cores are dense zones of molecular gas of relatively high density, and represent the physical and chemical conditions of interstellar gas just after or prior to localized gravitational collapse. These objects are essentially the seeds from which young stars may spring, and define the fundamental starting point of stellar evolution. Since PPIV (see *Langer et al.* 2000; *André et al.* 2000), enormous strides have been made in the observational characterization of such cores, thanks to the increased interest stemming from the promising early results reported at PPIV and to new instrumentation.

This review summarizes the advances made since PPIV, and, given the large number, it has been divided into two parts. In Part I (i.e., this chapter), we summarize major recent observational studies of the initial conditions of star formation, i.e., the individual physical and chemical properties of starless cores, with emphasis on cores not found in crowded regions. This subject includes their identification, morphologies, densities, temperatures, molecular abundances, and kinematics. In recent years, the internal density and temperature structures of starless cores have been resolved, regions of chemical depletion (or enhancement) have been studied, and inward motions have been measured. Part II of this review (see next chapter by *Ward-Thompson et al.*) summarizes what observed individual and group characteristics, including magnetic field properties,

mass distributions and apparent lifetimes, have taught us about the evolution of low-mass dense cores through protostellar formation. Despite significant progress, the observational picture of the earliest stages of star formation remains incomplete, and new observational and experimental data and theoretical work will be necessary to make further advances.

2. STARLESS CORES

2.1 Definition

Stars form within molecular gas behind large amounts of extinction from dust. This extinction has been used to locate molecular clouds (*Lynds*, 1962), isolated smaller clouds (*Clemens and Barvainis*, 1988), and particularly opaque regions within larger clouds (*Myers et al.*, 1983; *Lee and Myers* 1999). Locations within these clouds of relatively high density or column density, though identifiable from optical or infrared absorption (e.g., see chapter by *Alves et al.*), can also be detected using submillimeter, millimeter, or radio emission. For instance, spectroscopic studies of clouds found via extinction studies further selected those with evidence for dense gas (e.g., see *Myers et al.*, 1983; *Myers and Benson* 1983). These became known collectively as "dense cores," based primarily on whether or not they showed emission from NH_3, indicative of densities above about 10^4 cm^{-3} (*Benson and Myers*, 1989; see also *Jijina et al.*, 1999). Using IRAS data, *Beichman et al.* (1986) found that roughly half the known dense cores in clouds contained IRAS sources, while *Yun and Clemens* (1990) found that about 23% of the isolated smaller clouds contained infrared sources within; the remainder became known as "starless cores." Follow-up studies of clouds with sensitive submillimeter continuum detection systems allowed further discrimination within the class of starless cores. Those with detected emission, indicating relatively high densities of 10^{5-6} cm^{-3} (*Ward-Thompson et al.*, 1994), were called "pre-protostellar" cores or later "prestellar cores." Molecular line studies showed that prestellar cores were indeed more likely to show evidence for inflowing material than were the merely starless cores (e.g., see *Gregersen and Evans*, 2000).

In this review, we describe the recent observational characterization of "starless cores," low-mass dense cores without compact luminous sources of any mass. (We call such sources "young stellar objects," regardless of whether or not they are stellar or substellar in mass.) By "low-mass," we mean cores with masses $M < 10$ M$_\odot$, such as those found in the nearby Taurus or Ophiuchus clouds. Starless cores are important because they represent best the physical conditions of dense gas prior to star formation. Conceptually, we distinguish starless cores that are gravitationally bound as "prestellar cores" though it is very difficult to determine observationally at present whether a given core is bound or not (see below). In addition, we consider such cores as either "isolated" or "clustered" depending on the local surface density of other nearby cores and young stellar objects. Observations of isolated cores (e.g., *Clemens and Barvainis*, 1988) are easier to interpret since they generally inhabit simpler, less confused environments, i.e., without nearby cores or young stellar objects. Observations of clustered cores (e.g., *Motte et al.*, 1998) are important also because they are more representative of star formation within embedded clusters, i.e., where most stars form within the Galaxy (*Lada and Lada*, 2003). Finally, we describe cores as either "shielded" from or "exposed" to the interstellar radiation field (ISRF), depending on whether they do [e.g., many of those described by *Myers et al.*, 1983] or do not [e.g., those cataloged by *Clemens and Barvainis*, 1988] reside within a larger molecular cloud.

Observational limitations strongly influence how dense cores are defined. For example, low resolution data may reveal cores over a wide range of mass, but higher resolution data may reveal substructure within each, with their own range of (lower) mass, i.e., cores within cores. In addition, different tracers may probe different kinds of structure within clouds, due to varying density, temperature, or chemistry. Also, whether or not a given dense core contains a compact infrared-luminous source is ultimately a matter of observational sensitivity (e.g., L1014; see below). Finally, learning whether or not a given core is prestellar (i.e., gravitationally bound) requires accurate determination of its physical state (mass, temperature, and internal magnetic field). Masses alone can be uncertain by factors of $\sim$3 due to uncertainties in distances, dust opacities, molecular abundances, or calibration. Various new instrumentation of higher resolution and sensitivity will soon be available, making such observational characterization more tenable.

2.2 Identification

Observations of starless cores have focused mostly on examples within 1 kpc, where the highest mass sensitivities and linear resolutions are possible. Many starless cores have been detected serendipitously, adjacent to previously-known protostellar cores or young stellar objects (e.g., see *Wilson et al.*, 1999; *Williams and Myers*, 1999; *Swift et al.*, 2005). Only recently, more systematic mapping has begun to identify larger numbers of starless cores in less biased surveys.

Recent large line maps across significant portions of nearby molecular clouds using transitions that trace relatively high densities have been useful in identifying dense cores. For example, 179 cores in clouds within 200 pc were identified from substructure detected in C^{18}O (1–0) maps of L1333 in Cassiopeia (*Obayashi et al.*, 1998), Taurus (*Onishi et al.*, 1998), the Southern Coalsack region (*Kato et al.*, 1999), the Pipe Nebula region (*Onishi et al.*, 1999), Chamaeleon (*Mizuno et al.*, 1999), Lupus (*Hara et al.*, 1999), Corona Australis (*Yonekura et al.*, 1999), and Ophiuchus (*Tachihara et al.*, 2000). *Tachihara et al.* (2002) identified 76% of these cores as "starless" (i.e., without associated IRAS sources; see below) with masses of 1-100 M$_\odot$ (on average, 15 M$_\odot$). Using a still higher density molecu-

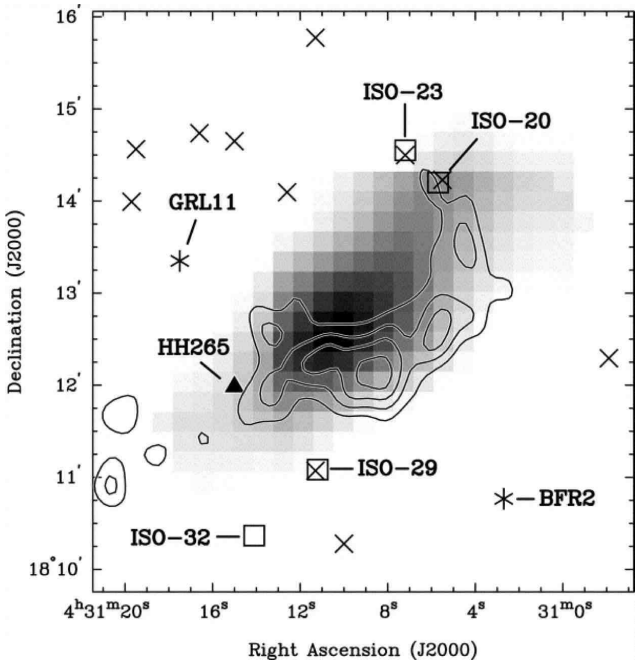

Fig. 1.— The prestellar core L1551-MC shown in NH_3 (1,1) integrated intensity (greyscale) and CCS(3_2–2_1) integrated intensity (contours). Positions of nearby objects are shown as symbols (see *Swift et al.*, 2005).

lar tracer, $H^{13}CO^+$ (1–0), *Onishi et al.* (2002) identified 55 "condensations" in Taurus, 80% of which were similarly deemed "starless" with estimated masses of 0.4-20 $M_\odot$. Using line maps to identify cores can be problematic, however, because of line optical depths and chemical evolution within the cloud. For example, lines like $C^{18}O$ (1–0) can be too opaque to sample most of the material in dense cores. Furthermore, this line and $H^{13}CO^+$ (1–0) can be affected by the significant depletion of the source molecules, again making it difficult to sample their column densities. In contrast, N–bearing molecules, in particular NH_3 and N_2H^+, appear to survive at higher densities than C-bearing species, and in fact they have been used to probe core nuclei (see *Caselli et al.*, 2002c; also Section 4).

Submillimeter or millimeter continuum emission maps of molecular clouds can trace the high column densities associated with starless cores without the potentially confusing effects of line opacity or chemical evolution. These studies trace the dust component, which emits radiation at long wavelengths even at the very low dust temperatures (T_D) in dense cores ($\sim$10 K), though the emission is sensitive to T_D. The optical properties of grains are also likely to evolve at relatively high densities due to ice mantle growth and coagulation, but these effects are much less severe than those for gas phase tracers (see Section 4). Recent single-dish telescope studies include the inner regions of Ophiuchus (*Motte et al.*, 1998; *Johnstone et al.*, 2000; *Johnstone et al.*, 2004; *Stanke et al.*, 2006), northern Orion A (*Chini et al.*, 1997; *Lis et al.*, 1998; *Johnstone and Bally*, 1999), NGC 2068/2071 in Orion B (*Mitchell et al.*, 2001; *Johnstone et al.*, 2001; *Motte et al.*, 2001), NGC 1333 in Perseus (*Sandell and Knee*, 2001), and R Corona Australis (*Chini et al.*, 2003; *Nutter et al.*, 2005). For example, *Motte et al.* (1998) found 58 "starless clumps" in their map of Ophiuchus with masses of 0.05-3 $M_\odot$. Even larger regions (e.g., 8–10 deg^2) have now been mapped (*Enoch et al.*, 2006; *Young et al.*, 2006; *Hatchell et al.*, 2005; *Kirk et al.*, 2006), providing expansive (though shallow) coverage of the Perseus and Ophiuchus clouds. Collectively these studies have revealed hundreds of compact continuum objects. In those cases where comparisons with near- to far-infrared data were made, more than $\sim$60% were deemed "starless." The fraction of these that are prestellar is not known, however, and determining this (through appropriate molecular tracers; see Section 4) is a key goal of future research.

In both line and continuum maps, the methods by which objects are identified have varied widely. Some studies have identified objects by eye, while others have used more objective automated structure identification algorithms (e.g., *Clumpfind* by *Williams et al.*, 1994), multiscale wavelet analyses, and even hybrid techniques. In addition, objects identified in continuum studies are significantly more compact in scale than those found in the line maps described above. First, angular resolutions of the data have substantially differed, with line and continuum maps typically having $> 1'$ and $< 1'$ resolutions respectively. Second, the spatial sampling of the data also have substantially differed, though single-dish telescopes were used for both. Line data are obtained through frequency or position switching to line-free locations, allowing large-scale information to be retained, but continuum data are obtained through chopping (or sky background removal for instruments that do not chop), filtering out large-scale information (e.g., over 2–10$'$ depending on the instrument.) Indeed, many continuum ob-

jects can be found embedded within objects identified via line surveys. Continuum cores have been identified, however, using relatively low-resolution data, e.g., from IRAS (*Jessop and Ward-Thompson*, 2000) or ISO (*Tóth et al.*, 2004).

Identification of objects found through line or continuum observations as starless cores is ultimately dependent upon the availability and sensitivity of ancillary data at the time of analysis. For example, Figure 1 shows the starless core L1551-MC in Taurus recently discovered by *Swift et al.* (2005) in NH_3 and CCS emission, with the positions of nearby, non-coincident objects listed in the SIMBAD database (as of late 2004). Far-infrared data from IRAS were used traditionally to find evidence for embedded protostars associated with detected cores, but more recently wide-field near-infrared data, including those from 2MASS, have been also used. Such wide-field data can be insufficiently sensitive to detect the youngest, most-embedded protostars, however, given high extinctions (e.g., $A_V > 30$). Near-infrared observations targeting specific cores can attain much higher sensitivities but these have not been done extensively. Some targeted studies, e.g., *Allen et al.* (2002) or *Murphy and Myers* (2003), however, did not detect low luminosity protostars in various cores despite relatively high sensitivity. The extraordinarily high sensitivity of the Spitzer Space Telescope in the mid-infrared has revealed about 12 low luminosity protostars within cores previously identified as starless, e.g., in L1014 by *Young et al.* (2004a) and in L1148 by *Kauffmann et al.* (2005; (see also *Bourke et al.*, in preparation; *Huard et al.*, in preparation). These are candidates to join the class of Very Low Luminosity Objects (VeLLOs), sources with $L_{int} < 0.1\ L_\odot$ that are located within dense cores. (Note that L_{int} is the luminosity of the object, in excess of that supplied by the ISRF.) Based on this definition, the previously identified, extremely young, low-luminosity Class 0 protostar IRAM 04191 (*André et al.*, 1999) is also a VeLLO (*Dunham et al.*, in preparation).

In addition to near- to far-infrared imaging, deeply embedded protostars may be identified using other signposts of star formation not affected by high extinction, including compact molecular outflows, "hot core" molecular line emission, masers, or compact thermal radio emission. For example, *Yun et al.* (1996) and *Harvey et al.* (2002) used the latter method to limit luminosities of protostellar sources within several starless cores using limits on radio emission expected from shock-ionized gas, i.e., from outflows.

3. DENSITY AND TEMPERATURE STRUCTURES

3.1 Probing Physical Structure

In this section, we describe the morphologies and internal configurations of density and temperature of starless cores as derived in recent studies. Much progress in understanding dense core structure has come from analyses of far-infrared to millimeter continuum emission observations, typically of relatively isolated and exposed examples. Continuum data have been used preferentially over molecular line data because interpretation of the latter can be complicated by large internal molecular abundance variations (see Section 4). Near- or mid-infrared absorption of background emission by cores can be also a powerful probe of the density structure since extinction is independent of temperature and can trace those locations where dust column densities are too low to be easily detected in emission at present (e.g., see *Bacmann et al.*, 2000). Results about core structure derived from "extinction mapping" have agreed generally with those from emission studies, with some exceptions (see below and the chapter by *Alves et al.*)

The observed emission from cores depends on the entangled effects of temperature, density, properties of the tracer being used, and the observational technique. For molecular lines, the abundance and excitation of the tracer varies within the core. For continuum emission from dust, the interpretation depends on dust properties and the characteristics of the ISRF. Two general approaches are taken: in the first, simplifying assumptions are made and the observations are inverted to derive core properties, usually averages over the line of sight and the beam; in the second, specific physical models are assumed and a self-consistent calculation of predicted observations is compared to the actual observations, allowing the best model to be chosen. Both approaches have their strengths and weaknesses.

Self-consistent models must compute the temperature distribution for a given density distribution, dust properties, and radiation field. For starless cores, only the ISRF heats the dust. In their models, *Evans et al.* (2001) included the "Black-Draine" (BD) ISRF, one based on the COBE results of *Black* (1994), which includes the cosmic microwave background (CMB) blackbody and the ISRF in the ultraviolet of *Draine* (1978; cf. *van Dishoeck* 1988), rather than the older, pre-COBE model of *Mathis et al.* (1983; MMP). The BD and MMP models can differ significantly, e.g., up to a factor of 13 between 5 μm and 400 μm. For dust opacities, those currently in use have been theoretically derived from optical constants of grain and ice materials and include features such as mid-infrared vibrational bands (e.g., 9.7 μm Si-O stretch) and tend toward a power-law decrease of opacity at submillimeter wavelengths ($\kappa_\nu \propto \lambda^{-\beta}$). Figure 2a shows five dust opacity models: OH5 and OH8 are models of grains that have coagulated for 10^5 yr and acquired varied depths of ice mantles (*Ossenkopf and Henning*, 1994); "Draine-Lee" are the "standard" interstellar medium dust opacities derived from silicate and graphite grains by *Draine and Lee* (1984); MMP opacities are derived from an empirical fit to observed dust properties in star-forming regions; and Pollack opacities are derived from an alternative grain composition based on silicate grains (olivine and orthopyroxene), iron compounds (troilite and metallic iron), and various organic C compounds (*Pollack et al.*, 1994). The mass opacity (κ_ν) at long wavelengths can vary by one order of magnitude between the opacity models.

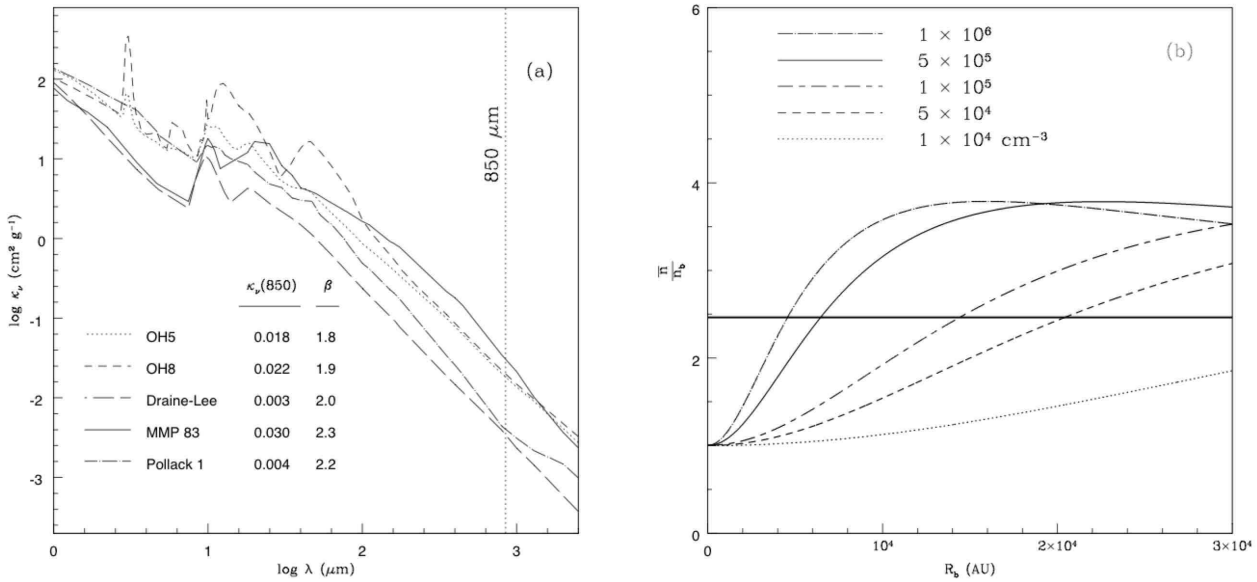

Fig. 2.— a) Opacity vs. wavelength from selected dust models (see Section 3.3; *Shirley et al.*, 2005). Values (κ_ν) and spectral indices (β) of opacities at 850 μm are tabulated. Units of κ_ν are cm^2 g^{-1} and the β at 850 μm were obtained from linear regressions of respective model values between 350 μm and 1.3 mm. b) The ratio of average density ($\bar{n}$) to density at the BES boundary radius (n_b) vs. BES boundary radius (R_b) for families of BES of given n_c (*Shirley and Jorgensen*, in preparation). The solid horizontal line corresponds to the stability criterion of *Lombardi and Bertin* (2001).

These ingredients then provide inputs to radiative transport codes (e.g., *Egan et al.*, 1988; *Ivezić et al.*,, 1999), which attempt to fit simultaneously the observed intensity profiles, $I_\nu(r)$ (most sensitive to variation in $n(r)$), and spectral energy distribution (SED, most sensitive to the total mass and the assumed dust opacity). To test various ISRF and dust opacity models for the L1498 starless core, *Shirley et al.* (2005) varied the BD ISRF by a scaling factor, s_{isrf}, and tested eight dust opacity models, including those shown in Figure 2a. In their models, the resultant SED was more sensitive to the ISRF than the resultant normalized continuum intensity profiles, and they found best fits with s_{isrf} = 0.5–1.0. Furthermore, only the OH5 and OH8 opacity models were consistent with the observed SED.

Chemical differentiation observed in starless cores (see Section 4) should lead to variations in ice compositions, and hence dust opacities. Indeed, *Kramer et al.* (2003) found in IC 5146 an increase in dust emissivity by a factor of 4 between 20 K and 12 K. To date, variations of dust opacity with radius have not been self-consistently included in radiative transfer models. Moreover, most radiative transfer models are 1D and are constrained by 1D intensity profiles, although starless cores can be quite ellipsoidal in 3D shape (see §3.2). If magnetic fields are dynamically important, they require core geometries that are inherently multidimensional since the magnetic field only provides support perpendicular to the direction of the field lines (e.g., *Li and Shu*, 1996). Promising work on modeling cores with 3D radiative transfer codes has begun (e.g., *Doty et al.*, 2005a, 2005b; *Steinacker et al.*, 2005). A reanalysis of L1544 core data by *Doty et al.* (2005a) using a 3D code yielded results that were overall similar to those found from 1D models but with reduced size and mass.

3.2 Morphology and Density Structure

Starless cores vary widely in morphology or shape, ranging between filamentary to compact and round. Cores are seen as 2D projections against the sky, making it difficult to constrain their 3D shape. Furthermore, core morphologies can depend on the wavelength and the angular resolution of observation (e.g., see *Stamatellos et al.*, 2004). Observed morphologies also depend upon the intensity level chosen as the boundary between cores and their surroundings, and this can be affected strongly by observational sensitivity. In general, cores that are round (in projection) have been typically interpreted as being spherical in shape, while cores that are elongated (in projection) have been typically interpreted as being either oblate or prolate spheroids. Statistical analyses of core map aspect ratios indicate that most isolated cores are prolate rather than oblate (*Myers et al.*, 1991; *Ryden*, 1996), and many cores in Taurus share the projected alignment of the filamentary clouds in which they reside (*Hartmann*, 2002). *Jones et al.* (2001), using a sample of cores identified from the extensive NH_3 catalog of *Jijina et al.* (1999), posited that elongated cores actually have intrinsically triaxial shapes that are neither purely oblate nor prolate. *Goodwin et al.* (2002), using the same catalog, found starless cores have more extreme axial ratios than protostellar cores.

Column densities within starless cores can be traced using the optically thin millimeter or submillimeter continuum specific intensity. Derivation of absolute column den-

sities and conversion to volume densities requires knowledge or assumptions about dust temperatures, opacities, gas-to-dust ratios, geometry, and telescope beam pattern. Azimuthally averaged (or elliptically averaged in cases of extreme axial ratio), 1D intensity profiles of starless cores are found to have "flat" slopes at radii $<$ 3000-7500 AU and "steep" slopes at larger radii (see *Ward-Thompson et al.*, 1994; *André et al.*, 1996; *Ward-Thompson et al.*, 1999; *Shirley et al.*, 2000; *Kirk et al.*, 2005). Such profiles depart from the $n(r) \propto r^{-2}$ distribution of the "singular isothermal sphere" postulated by *Shu* (1977) as the initial state of isolated dense cores prior to gravitational collapse. Similar profiles have been seen also in studies of dense core structure utilizing the absorption of background emission by core dust (e.g., *Alves et al.*, 2001; see chapter by *Alves et al.*) The observed configurations are better described by "Bonnor-Ebert spheres" (BES; *Emden*, 1907; *Ebert*, 1955; *Bonnor*, 1956; *Chandrasekhar*, 1957), non-singular solutions to the equations of hydrostatic equilibrium that can be critically stable in the presence of external pressure. In the 1D isothermal approximation, the family of BES solutions are parameterized by the central density, n_c, and are characterized by density profiles with two regimes: a "plateau" of slowly decreasing density at small radii and a power-law decrease ($\sim r^{-2}$) at large radii (*Chandrasekhar and Wares*, 1949). The size of the plateau scales inversely with the central density, i.e., $R(\frac{1}{2}n_c) \propto \sqrt{T/n_c}$. For reference, Figure 2b shows the average density contrast, $\frac{\bar{n}}{n_b}$, where $\bar{n}$ is the average density and n_b is the density at the BES (outer) boundary radius, versus BES boundary radius, R_b, for families of BES of given n_c (*Shirley and Jorgensen*, in preparation). Thermally supported density configurations, regardless of geometry, are unstable if they have $\frac{\bar{n}}{n_b} \geq 2.46457$ (*Lombardi and Bertin*, 2001). Such configurations may remain stable if non-thermal internal pressures (e.g., from magnetic fields or turbulence) are relevant, however; see Section 5, as well as the next chapter by *Ward-Thompson et al.*

Detailed modeling of continuum intensity profiles have confirmed that BES are a good approximation to the density structures of starless cores (e.g., *Ward-Thompson et al.*, 1999; *Evans et al.*, 2001; *Kirk et al.*, 2005; *Schnee and Goodman*, 2005, but see *Harvey et al.*, 2003). Recently, *Shirley and Jorgensen* (in preparation) modeled submillimeter continuum emission from 33 isolated starless cores, the largest sample so far, and found a log-normal distribution of central densities with median $\log n_c$ = 5.3 cm^{-3}. This large median central density indicates that non-thermal support (e.g., magnetic pressure) has stabilized the cores, that the density scale is inaccurate due to the dust opacity assumed (see below), or that these cores are not in equilibrium. Unfortunately, it is not currently possible to distinguish between collapsing and static BES with dust emission or absorption profiles because the density structure, for a given n_c, does not significantly vary until late in the collapse history (*Myers*, 2005). Molecular probes of the kinematics are much better suited to resolving this issue (e.g., see Section 5). Nevertheless, increasing central concentration within starless cores could indicate an evolutionary path. Note, however, that while BES are consistent with current observations, this does not prove that given physical structures *are* BES (cf. *Tafalla et al.*, 2002; *Ballesteros-Paredes et al.*, 2003, but see Section 5.2).

3.3 Temperature Structures

Early calculations of dust temperature (T_D) in cores heated only by the ISRF indicated $T_D \sim 10$ K (*Leung*, 1975), cooler on the inside and warmer on the outside. Such a gradient in T_D is unavoidable theoretically because the cores are optically thin to their own radiation ($\lambda_{\rm peak} \approx 200$ μm) and are primarily heated externally by a local ISRF for which short wavelength radiation is significantly obnubilated in the center of the core. Alternative heating mechanisms for dust, including cosmic rays (i.e., direct heating of grains, secondary UV heating from excitation of H_2, and heating of gas followed by gas-grain heating) are not significant compared to heating from the ISRF. More recent calculations using current ideas for the ISRF and dust opacites confirm the earlier work (e.g., *Zucconi et al.*, 2001; *Evans et al.*, 2001), finding T_D falling from about 12 K on the exposed surface to as low as 7 K at very small radii. Such low temperatures would suppress radiation even at millimeter wavelengths from the center, possibly affecting interpretation of the central densities. Gradients of T_D found in starless cores, however, do not have a strong effect on overall core equilibria, and density profiles very different from isothermal BES are not expected (*Evans et al.*, 2001; *Galli et al.*, 2002).

The temperature gradient within a core depends on the strength and spectral properties of the ISRF, which are affected by surrounding extinction, and the density structure in the core. Shielded cores have lower temperatures and shallower gradients than exposed cores, because the ISRF is attenuated and reddened (*Stamatellos and Whitworth*, 2003; *André et al.*, 2003; *Young et al.*, 2004b). The reddening leaves more of the heating to the longer wavelength photons, which "cook" more evenly. Cores of relatively low central concentration or low central density should have shallower temperature gradients due to lower extinction (*Shirley et al.*, 2005). Calculations in higher dimensions also show smaller gradients. For clumpy cores, the heating is dominated by unobscured lines of sight (*Doty et al.*, 2005b). Such clumpy cores can have cold patches ($T_D < 6$ K) within an overall flatter distribution of T_D.

Observational tests do indicate warmer T_D on the outside of cores. *Langer and Willacy* (2001), *Ward-Thompson et al.* (2002) and *Pagani et al.* (2004, see also 2003), each using ISO data, found evidence for T_D gradients in exposed cores, with innermost $T_D \leq 10$ K. Limited spatial resolution at far-infrared wavelengths, however, does not allow direct tests of the predictions of very low T_D at very small radii. One indirect test comes from studies of starless cores in extinction (e.g., *Bacmann et al.*, 2000), which are tem-

perature independent. These studies also show "flat" inner density gradients, and hence these gradients are not due to decreased T_D in the centers. Another possible indirect test is the high-resolution study of molecular lines (see below).

Examining gas kinetic temperature (T_K), *Goldreich and Kwan* (1974) showed it is forced to be very close to T_D at high densities ($n \geq 10^5$ cm^{-3}). This coupling fails for less dense cores and for the outer parts of even denser cores (*Goldsmith*, 2001; *Galli et al.*, 2002). At first, T_K may drop below T_D, but cosmic ray heating prevents T_K from dropping too low. If the core is not very deeply shielded, however, photoelectric heating causes $T_K > T_D$ in the outer layers (e.g., *Young et al.*, 2004b).

Reductions in the ISRF affect the chemistry in the outer layers (*Lee et al.*, 2004b) and change the gas kinetic temperature (T_K) profile as well by decreasing photoelectric heating. Conversely, cores in regions of high ISRF will have warmer surfaces in both dust and gas (*Lis et al.*, 2001; *Jørgensen et al.*, 2006). Since this heating is caused by ultraviolet light, it is very sensitive to small amounts of shielding. CO is a particularly good constraint on the short-wavelength end of the ISRF (e.g., *Evans et al.*, 2005), but, with chemical models (Section 4) other species can also be excellent probes (e.g., *Young et al.*, 2004b; *Lee et al.*, 2004b).

Observationally, T_K can be determined directly from CO transitions, which probe the outer layers, and by inversion transitions of NH_3, a good tracer of dense core material (e.g., see *Jijina et al.*, 1999 and references therein), which probe deeper layers. Analyses of such lines from starless cores have found nearly constant values of $T_K \approx$ 10 K (e.g., *Hotzel et al.*, 2002 for B68 and *Tafalla et al.*, 2004 for L1498 and L1517B). If $T_K = T_D$, and T_D decreases toward the center, one might expect to see changes in T_K. For L1498 and L1517B, however, *Galli et al.* (2002) found T_K was $\sim$2 K higher than T_D for cores with central densities $\sim 10^5$ cm^{-3} (i.e., like L1498 and L1517B), and that neither T_K nor T_D varied significantly within the inner core radii. *Shirley et al.* (2005), however, found a much lower central density (i.e., $n_c = 1 - 3 \times 10^4$ cm^{-3}) for L1498, which would explain the difference of T_K and T_D. Also, recent VLA observations of NH_3 (1,1) and (2,2) across the L1544 prestellar core by *Crapsi et al.* (in preparation) have revealed a clear T_K gradient that is consistent with the dust temperature profile derived from models of submillimeter continuum emission with a central density of 3×10^6 cm^{-3}.

4. CHEMICAL CHARACTERISTICS

Structures of starless cores in principle can be probed using molecular emission lines, typically rotational transitions excited at the relatively low temperatures and high densities of such objects. Indeed, line data can complement continuum data to provide new constraints to models (e.g., *Jessop and Ward-Thompson*, 2001). Line studies also have the advantage of tracing kinematic behavior of starless cores. In practice, however, line observations are affected by the abundance variations within the cores and by the optical depths of the specific lines used; unlike submillimeter or millimeter continuum emission, the optical depths of molecular lines are often quite large. To circumvent this problem, lines from rare isotopologues are observed and interpreted using non-LTE radiative transfer codes, which take into account the core chemical structure.

Although the basic chemical processes in clouds have been known for some time (e.g., formation of H_2 on dust grains (*Gould and Salpeter*, 1963; *Jura*, 1975), ionization of H_2 by cosmic rays (*Solomon and Werner*, 1971), ion–molecule reactions (*Herbst and Klemperer*, 1973), and grain-surface chemistry (*Watson and Salpeter*, 1972; *Allen and Robinson*, 1977)), there are still several uncertainties for denser regions, one of which is grain-surface processes. Theoretical studies predicted molecular depletion onto grain surfaces (e.g., *Léger*, 1983). While adsorbed molecules have long been observed in infrared absorption bands (e.g., *Gillett and Forrest*, 1973; see also *Pontoppidan et al.*, 2005), only in the past few years have molecular line observations found clear and quantitative evidence for gas-phase depletion (e.g., *Kuiper et al.*, 1996; *Willacy et al.*, 1998; *Kramer et al.*, 1998, see Section 4.1). Enhanced deuterium fractionation, which should accompany molecular depletion (e.g., *Brown and Millar*, 1989), is also found in both starless and protostellar cores (see Section 4.2). Uncertainties still remain, however, and further updates of chemical models and detailed comparisons with new observational data are needed.

4.1 Molecular Freeze-out

The dominant gas phase constituent in molecular clouds is H_2 but its line emission is not used to trace the interiors of molecular clouds and cores. H_2, as a homonuclear molecule, has no electric dipole moment and thus has no dipole transitions between rotational states. Quadrupole emission between states is possible but the upper level of the first allowed transition is 512 K above ground (since H_2 is a light molecule) and is only excited where gas is suitably hot, e.g., on cloud surfaces and not in cloud interiors.

CO and its isotopologues ^{13}CO, C^{18}O or C^{17}O are commonly used as surrogate tracers to H_2 since they are relatively abundant and intermixed with H_2, and have rotational transitions excited at the ambient densities in molecular clouds, i.e., 10^{2-3} cm^{-3}. Recent studies, however, have found significant depletions of CO abundance within the innermost regions of starless cores by comparing line observations of CO isotopologues with the submillimeter dust continuum or extinction maps of cores. For example, *Bacmann et al.* (2002) found evidence for CO depletions by factors of 4-15 in a sample of 7 cores. Furthermore, *Caselli et al.* (1999) and *Bergin et al.* (2002), using C^{17}O and C^{18}O respectively, found CO abundance depletions by factors of $\sim$1000 and $\sim$100 in the centers of the L1544 and B68 cores respectively, i.e., where $n \geq 10^5$ cm^{-3}.

The most common explanation for these abundance variations is that CO and its isotopologues adsorb, i.e., "freeze-out," easily onto grain mantles at high densities and dust temperatures < 20 K. Other molecules are also similarly depleted onto dust grains within low-mass cores. For example, *Bergin et al.* (2001), *Young et al.* (2004b), *Lai et al.* (2003) and *Ohashi et al.* (1999) found observational evidence for depletions of CS, H_2CO, C_3H_2 and CCS respectively toward various dense cores. More recently, *Tafalla et al.* (in preparation) carried out a multimolecular study of the L1498 and L1517B cores and found evidence for the depletion of 11 species, including all the aforementioned species plus DCO^+, HCN, HC_3N, HCO^+, CH_3OH and SO.

Water is also clearly frozen onto dust grains. First, solid water is seen (with abundances $\sim 10^{-4}$ relative to H_2) in absorption within the near-infrared spectra of stars located behind molecular clouds and those of embedded protostars (e.g., *van Dishoeck*, 2004 and references therein). Indeed, water ice is the major compound of grain mantles, followed by CO (e.g., *Chiar et al.*, 1995; *Ehrenfreund and Charnley*, 2000). Second, the recent SWAS mission furnished stringent upper limits to abundances of water vapor ($<10^{-8}$ relative to H_2; *Bergin and Snell* 2002) that are orders of magnitude lower than values predicted by gas–phase chemical models that did not account for the gas–grain interaction and the consequent molecular freeze-out. Other ices on grain surfaces recently detected through absorption spectra of background stars include CO_2 (*Bergin et al.*, 2005), and probably HCOOH and NH_4^+ (*Knez et al.*, 2005).

The degree to which a given molecule depletes onto grains is likely a function of its respective binding energy onto grain surfaces, but other chemical factors may be also important. For example, carbon-chain molecules such as CCS and C_3H_2, which are called "early-time" species because in gas–phase chemical models they form before atomic carbon is mainly locked in CO (*Herbst and Leung*, 1989), can decrease in abundance due to gas-phase reactions, especially with atomic oxygen, which tend to convert all C-bearing species into CO. When CO and the reactive O start to freeze-out, carbon-chain species increase their abundance again, showing a "late-time" secondary peak, limited in time by their own adsorption onto grains (*Ruffle et al.*, 1997, 1999; *Li et al.*, 2002; *Lee et al.*, 2003).

Nitrogen-bearing molecules, e.g, NH_3 and N_2H^+, have been shown to be quite resilient tracers of dense cores, relative to carbon-bearing molecules. They are called "late-time" species; they both have N_2 as a parent molecule, which forms slowly (relative to CO) in the gas phase via neutral-neutral reactions. As described in Section 2, NH_3 transitions have long been tracers of dense cores since these can be excited at densities $\approx 10^4$ cm^{-3}. In recent years, however, N_2H^+ transitions have grown in popularity for tracing dense cores with surveys by *Benson et al.* (1998), *Caselli et al.* (2002c) and *Tatematsu et al.* (2004). The intensity distribution of N_2H^+ 1–0 in a given core closely matches that of the millimeter or submillimeter continuum (e.g., *Caselli et al.*, 2002a) and its hyperfine structure can be fit to determine excitation temperatures and line opacities (under the assumption that all the hyperfine components have the same excitation temperature; see *Womack et al.* 1992; *Caselli et al.* 1995). Within 5 cores, *Tafalla et al.* (2002; see also *Tafalla et al.*, 2004) found inner zones of CO and CS depletion by factors ≥ 100 but NH_3 abundances that increased by factors of $\sim$1-10 towards the core centers and constant N_2H^+ abundances.

The relatively high abundances of NH_3 and N_2H^+ in starless cores were thought to be due to the low binding energy of their parent N_2 relative to CO (*Bergin and Langer*, 1997), but recent laboratory experiments by *Öberg et al.* (2005; see also *Bisschop et al.*, 2006) have found the binding energies to be quite similar. Another possible explanation is a slow formation of N_2 molecule in the gas phase (*Caselli and Aikawa*, in preparation). In the initial formation of molecular clouds, the N atom would be the dominant form of nitrogen. The nitrogen atom has a lower adsorption energy than N_2 and CO, and thus is more resilient to adsorption. Formation of N_2 is much slower than the CO formation in the gas phase, and hence many N atoms are still available when the adsorption starts (i.e., when the core age exceeds the collisional timescale between gas and dust). Adsorption of N_2 is compensated by the formation in the gas phase. The high abundance of their mother molecule helps N_2H^+ and NH_3 to maintain their abundances. Two additional factors lead to high N_2H^+ abundance. First, N_2H^+ does not directly adsorb onto grains; it recombines on charged grain surfaces and returns to the gas-phase as N_2. Second, the main reactants of N_2H^+, e.g., CO and electrons, decrease as the core density rises. Indeed, in Model A of *Aikawa et al.* (2001), depletion of N_2H^+ and NH_3 is much less significant than that of CO, even though the adsorption energies of CO and N_2 are assumed to be equal. The central NH_3 enhancement relative to N_2H^+ can be caused by CO depletion. In the outer regions with high CO abundance, N_2H^+ mainly reacts with CO to produce N_2, while, in the central regions with heavy CO depletion, it recombines to produce NH as well as N_2 (*Geppert et al.*, 2004), which is transformed to NH_3 (*Aikawa et al.*, 2005).

Nitrogen-bearing species are not immune to depletion and even N_2 will be eventually adsorbed onto grains at high densities in starless cores (e.g., *Bergin and Langer*, 1997; *Aikawa et al.*, 2001). *Bergin et al.* (2002) and *Crapsi et al.* (2004) found evidence for small zones of N_2H^+ depletion (by factors of $\sim$2) coincident with the centers of the exposed cores in B68 and L1521F, respectively. In addition, *Di Francesco et al.* (2004) and *Pagani et al.* (2005) found evidence for N_2H^+ depletion in the Oph A and L183 cores, respectively. *Belloche and André* (2004) and *Jørgensen et al.* (2004) found N_2H^+ depletion within cold IRAM 04191 and NGC 1333 IRAS 2 protostellar cores respectively, but outflows may have also partially affected the local chemistry if CO has been released from grain mantles near the protostars. Further, *Caselli et al.* (2003) and *Walmsley et al.* (2004) have suggested that all molecules with C, N or O can be utterly depleted in the innermost regions of denser

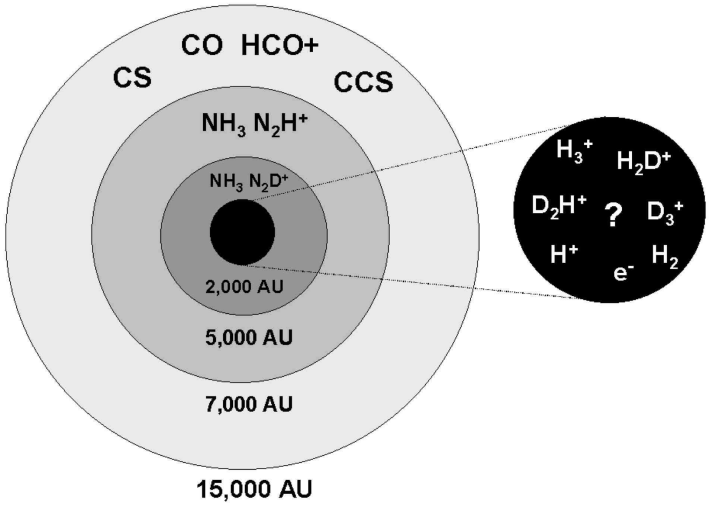

Fig. 3.— A schematic representation of eventual molecular differentiation within a starless core. The external shell of the core (where $n(\mathrm{H_2}) \simeq 10^4$ cm^{-3}) can be traced by CO, CS and other carbon bearing species. At radii < 7000 AU, where $n(\mathrm{H_2}) \simeq 10^5$ cm^{-3}, CO and CS disappears from the gas phase and the best gas tracers are NH_3 and N_2H^+. At higher densities, deuterated species become quite abundant and, when the density exceeds $\sim 10^6$ cm^{-3}, the chemistry will be dominated by light molecular ions, in particular H_3^+ and its deuterated forms, as well as H^+ (e.g., *Walmsley et al.*, 2004).

cores based on interpretation of the H_2D^+ emission in the L1544 core. Indeed, molecules without heavy elements, e.g., H_2D^+, may be the only remaining molecular tracers of such regions.

Figure 3 schematically summarizes how the eventual molecular differentiation within a starless core may look. At radii of ∼7000-15000 AU, CO and CS are still mainly in the gas phase and the main molecular ion is HCO^+, with which one can deduce a stringent lower limit of the electron density (e.g., Caselli et al., 1998; see Section 4.3). The fraction of atomic carbon in the gas is still large, as testified by the large observed abundances of carbon–chain molecules, such as CCS (e.g., *Ohashi et al.*, 1999). Deeper in the core (∼5000-7000 AU), where the density approaches values of the order of 10^5 cm^{-3}, CO and CS disappear from the gas–phase because of the freeze–out onto dust grains. The physical and chemical properties (as well as kinematics) are better traced by N–bearing species, in particular NH_3. Within the central 5000 AU, deuterium fractionation takes over (see Section 4.2), and N_2D^+ becomes the best probe (*Caselli et al.*, 2002a). NH_3 is still abundant in these regions, however, as suggested by the observed increase of the NH_3 abundance toward core centers (*Tafalla et al.*, 2002). At $r \leq 2500$ AU, where $n(\mathrm{H_2}) \geq 10^6$ cm^{-3}, all neutral species are expected to freeze–out in short time scales ($\leq$1000 yr) and light species, such as H_3^+ and its deuterated forms are thought to dominate the chemistry and the degree of ionization (*Caselli et al.*, 2003; *Vastel et al.*, 2004).

The schematic picture of Figure 3 of course depends on the time spent by a starless core in this condensed phase, so that one expects to find less significant depletion and more typical cloud chemistry in those objects that just entered this phase (e.g., possibly the L1521E core; see *Tafalla and Santiago*, 2004). Moreover, recent VLA observations of NH_3 (1,1) and (2,2) by *Crapsi et al.* (in preparation) have shown that NH_3 is still present in the central 800 AU of the L1544 core, where the gas density is a few times 10^6 cm^{-3}. If no efficient desorption mechanisms are at work, the time spent by the L1544 core nucleus in its high density phase may be < 500 yr (see Section 4.4). More examples are needed to refine chemical models of starless cores.

4.2 Deuterium Fractionation

Another important chemical process recently identified within starless cores is deuterium fractionation, i.e., the enhancement of deuterated isotopologues beyond levels expected from the elemental D/H ratio of $\sim 1.5 \times 10^{-5}$ (*Oliveira et al.*, 2003). For example, in a sample of dense cores, *Bacmann et al.* (2003) found a D_2CO/H_2CO column density ratio between 0.01 and 0.1. In addition, *Crapsi et al.* (2005) found N_2D^+/N_2H^+ ratios between 0.05 and 0.4 in a similar sample of cores. Deuterium fractionation is related to core temperature and CO depletion (e.g., *Dalgarno and Lepp*, 1984). Species such as H_3^+ and CH_3^+ are enriched in deuterium in cold clouds because of the difference in zero-point energies between deuterated and non-deuterated species and rapid exchange reactions such as $H_3^+ + HD \rightarrow H_2D^+ + H_2$ (e.g., *Millar et al.*, 1989). The enrichments are propagated to other molecules by chemical reactions. At high densities, heavy element molecules like CO will also

deplete onto grains, reducing the destruction rate of H_2D^+ and further increasing the H_2D^+/H_3^+ ratio. For example, the N_2D^+/N_2H^+ ratio is higher than the DCO^+/HCO^+ ratio by a factor of about 5 in the L1544 core (*Caselli et al.*, 2002b) because N_2H^+ can trace the central region with CO depletion, while HCO^+, which is produced by the protonation of CO, is not abundant at the core center.

Multiply deuterated species, such as HD_2^+ and D_3^+, can be similarly increased in abundance (*Roberts et al.*, 2003; see the chapter by *Ceccarelli et al.*). For example, the L1544 and IRAS 16293E core centers are also rich in H_2D^+ and HD_2^+, as confirmed respectively by *Caselli et al.* (2003) and *Vastel et al.* (2004).

The sensitivity of the D/H ratio to physical conditions and molecular depletion could make it a potentially useful probe of chemical or dynamic evolution of cores. For example, *Crapsi et al.* (2005) observed 14 cores and found that deuterium enhancement was higher in those that are more centrally concentrated and have larger peak H_2 and N_2H^+ column densities, i.e., arguably those more likely to collapse into stars.

4.3 Fractional Ionization

Observation of molecular ions, combined with chemical models, are used frequently to derive ionization degree, x_e. This value is important for dynamics since the amounts of free charge within cores determine the relative influence on core evolution of ambipolar diffusion, the gravitational inward motion of neutral species retarded by interactions with ionic species bound to a strong magnetic field (e.g., see *Ciolek and Mouschovias*, 1995). For example, *Caselli et al.* (1998; see also *Williams et al.*, 1998) found, for dense cores observed in DCO^+ and HCO^+, x_e values between 10^{-8} and 10^{-6}, with associated ambipolar-diffusion/free-fall timescale (AD/FF) ratios of 3-200 and no significant differences between starless and protostellar cores. In the L1544 core, using N_2D^+ and N_2H^+, *Caselli et al.* (2002b) found a significantly smaller x_e, $\sim 10^{-9}$, and an associated AD/FF ratio of $\sim$1, suggesting this particular core is near dynamical collapse.

Estimates of x_e, however, depend on many assumptions, e.g., the cosmic-ray ionization rate and molecular depletion degrees, as well as the accuracy of the chemical models used. In particular, the cosmic–ray ionization rate, ζ, typically assumed to be around 1–3 $\times$ 10^{-17} s^{-1} in molecular clouds (e.g., *Herbst and Klemperer*, 1975; *van der Tak and van Dishoeck*, 2000), seems to be closer to 10^{-15} s^{-1} in diffuse clouds (*McCall et al.*, 2003). Therefore, a large variation of ζ is expected in the transition between diffuse and molecular clouds (e.g., *Padoan and Scalo*, 2005) and, maybe, between dense cores with different amounts of shielding. Such variation may, in turn, cause significant variations of the ionization degree between cores (e.g., *Caselli et al.*, 1998) with consequent differences in AD/FF time scales. *Padoan et al.* (2004) have further argued that the ISRF strengths (i.e., A_V) and core age variations may account for at least some of the large range of x_e seen in dense cores. *Walmsley et al.* (2004) and *Flower et al.* (2005) have also suggested that the charge and size distributions of dust grains impact ionic abundances, and thus the local AD/FF ratio, in the centers of cores depleted of heavy-element species.

4.4 "Chemodynamical" Evolution

Depletions or enhancements of various molecular species in starless cores can be used as probes of dynamical evolution, since chemical and dynamical timescales can significantly differ. For example, if the dynamical timescale of a core is shorter than the adsorption timescale of CO ($\sim 10^4 (\frac{10^5 [\mathrm{cm}^{-3}]}{n(\mathrm{H}_2)}) (\frac{10[\mathrm{K}]}{T_{\mathrm{gas}}})^{0.5}$ yr), it will not experience CO depletion. Recent theoretical studies have investigated the evolution of molecular abundance distributions in cores (e.g., in L1544) using models including Larson-Penston collapse, ambipolar diffusion of magnetized cores, and contraction of a critical BES (*Aikawa et al.*, 2001, 2003, 2005; *Li et al.*, 2002; *Shematovich et al.*, 2003; *Lee et al.*, 2004b), showing that chemistry can be used to probe, although not uniquely, how the core contracts.

It is important to note that not all starless cores display similar chemical differentiation. *Hirota et al.* (2002) found that CCS is centrally peaked in the L1521E core, while it is depleted at the center of the L1498 core (*Kuiper et al.*, 1996), although the central density of the L1521E core ($\sim$3 $\times$ 10^5 cm^{-3}) is *higher* than that of the L1498 core ($\sim$1 $\times$ 10^{4-5} cm^{-3}; see *Shirley et al.*, 2005; *Shirley and Jorgensen*, in preparation; *Tafalla et al.*, 2002, 2004, 2005). The L1521E core also has low NH_3 and N_2H^+ abundance, low DNC/HNC ratio, and no CO depletion (*Hirota et al.*, 2001, 2002; *Tafalla and Santiago*, 2004). The core is apparently "chemically young"; these molecular abundances are reproduced either at early stages of chemical evolution in a pseudo-time dependent model (i.e., assuming that the density does not vary with time), or in a dynamical model where the contraction or formation timescale of a core is smaller than the chemical timescale (e.g., *Lee et al.*, 2003; *Aikawa et al.*, 2001; 2005). Other candidates of such "chemically young" cores are those in L1689B, L1495B, and L1521B (*Lee et al.*, 2003; *Hirota et al.*, 2004). Further determinations of kinematics and physical conditions in these cores and "chemically old" cores (e.g., that in L1498) will be very useful toward understanding chemical evolution in starless cores.

5. BULK AND TURBULENT MOTIONS

5.1 Bulk Motions

Molecular line profiles can be effective tracers of starless core kinematics, provided appropriate lines are observed and modeled. For example, internal velocity gradients in dense cores can be derived from the variation of line profiles across cores. Recent interpretations of such gradients as rotational in origin include those made by *Barranco and*

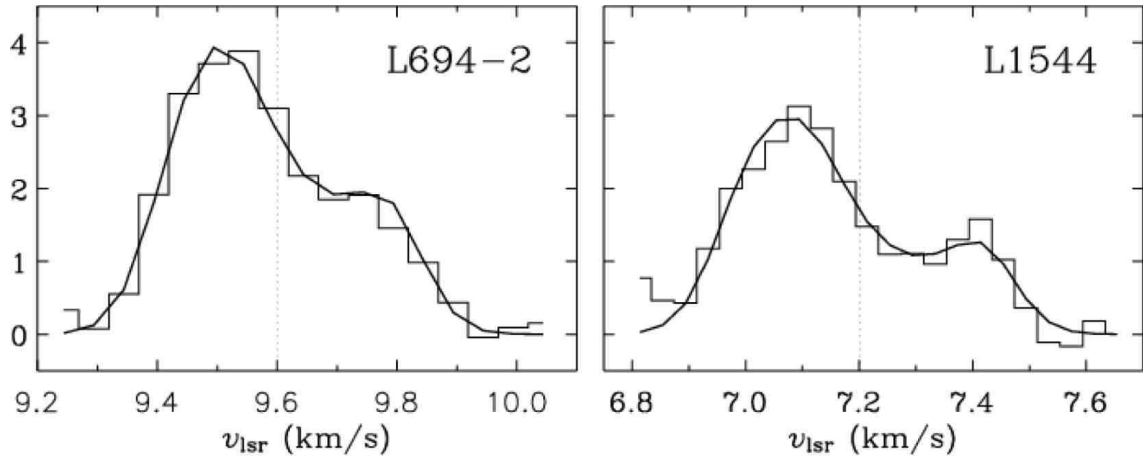

Fig. 4.— Spectra of the F1,F = 2,3→1,2 hyperfine component of N_2H^+(1–0) (histograms) from the starless cores in L694-2 (left) and L1544 (right) from *Williams et al.* (2006). Each spectrum is an average of emission within the central $10''$ of each core. Each profile, asymmetrically blue with respect to the systemic velocity of each core (dotted lines), is indicative of inward motions, and can be reproduced well with a two-layer radiative transfer model (solid curves).

Goodman (1998) of NH_3 (1,1) emission over 3 isolated starless cores, finding velocity gradients of ∼0.3 to 1.40 km s^{-1} pc^{-1} with projected rotational axes not aligned along projected core axes. In addition, *Swift et al.* (2005) found a 1.2 km s^{-1} pc^{-1} gradient of NH_3 emission aligned with the minor axis of the isolated starless core L1551-MC (see Figure 1). Furthermore, *Lada et al.* (2003) found evidence for differential rotation and angular momentum evolution in the B68 core, finding velocity gradients of 3.4 km s^{-1} pc^{-1} and 4.8 km s^{-1} pc^{-1} from $C^{18}O$ (1–0) and N_2H^+ (1–0) emission respectively, which in turn likely trace outer and inner core material respectively.

Further investigations of velocity gradients include a study of 12 starless and 14 protostellar cores mapped in N_2H^+ (1–0) by *Caselli et al.* (2002c), who derived a typical velocity gradient of 2 km s^{-1} pc^{-1} for both types of cores, and found that the spatial variations of the gradients indicate complex motions not consistent with simple solid body rotation. As found in the earlier study of cores by *Goodman et al.* (1993), these motions appear dynamically insignificant, since the derived rotational energies are at most a few percent of the respectively derived gravitational potential energies. Even relatively small rotational energies, however, could influence protostellar formation during core collapse. For example, angular momentum evolution due to contraction (see below) may induce disk formation or fragmentation into multiple objects (e.g., see *Hennebelle et al.* 2004).

In addition to plane-of-sky motions, molecular line profiles can be used to trace the gas kinematics along the line-of-sight. For example, *Walsh et al.* (2004) determined that the relative motion between 42 isolated cores and their surrounding gas was relatively low (e.g., $\leq$ 0.1 km s^{-1}) by comparing profiles of a core tracer like N_2H^+ with profiles of cloud tracers like $C^{18}O$ and ^{13}CO. This result implies that cores do not move ballistically with respect to their surrounding gas.

Molecular line profiles can also be used to detect inward motions in cores. Such motions can be detected using optically thick lines, which will appear asymmetrically blue relative to symmetric, optically thin lines in a centrally contracting system. Indeed, inward motions may distinguish prestellar cores from starless ones, since they may indicate gravitational binding (see Section 2.1; *Gregersen and Evans*, 2000; *Crapsi et al.*, 2005). Asymmetrically blue profiles were reproduced very well in collapse models of the protostellar envelope of B335 by *Zhou et al.* (1993), *Choi et al.* (1995), and *Evans et al.* (2005). In those protostellar cases, the models indicated that the self absorption is due to the static envelope expected in the inside-out collapse (*Shu*, 1977) and the blue peak is stronger because of radiative transfer effects (see *Zhou et al.*, 1993). Although such profiles may in principle also arise from rotational or outflow motions, 2D mapping and detailed modeling of the emission can distinguish between the different cases (e.g., *Narayanan and Walker*, 1998; *Redman et al.*, 2004). In addition, explanations other than inward motions would not favor blue-skewed over red-skewed profiles in a statistical sample.

Figure 4 shows two examples of such profiles, seen in the F_1,F = 2,3 → 1,2 hyperfine component of the N_2H^+ (1–0) transition, observed towards the central positions of the L694-2 and L1544 starless cores from *Williams et al.* (2006). Such a blue-skewed profile results from red-ward self-absorption, i.e., absorption along the line-of-sight by foreground, inward-moving gas of lower excitation. The statistics and the extended nature of many of the blue profiles suggest that inward motions exist before formation of the central luminosity source, in contrast to predictions of the simplest inside-out collapse models (e.g., *Shu*, 1977).

Such blue-skewed line profiles can be modeled with radiative transfer codes to estimate inward motion velocities. A simplified solution to the problem has been presented by

Myers et al. (1996) with a "two-layer" model, i.e., with two isothermal gas layers along the line-of-sight approaching each other, that can be used to determine rapidly the essentials of inward velocity. Figure 4 shows how well such modeling can reproduce observed asymmetrically blue profiles, with infall velocities of $\sim$0.1 km s^{-1} for both cores. With the same goal, *De Vries and Myers* (2005) have recently provided a more realistic "hill" model, i.e., where the excitation increases with optical depth along the line-of-sight. Full radiative transfer solutions, on the other hand, can now be obtained relatively rapidly, and can be used to derive velocities (as well as densities, temperatures, and molecular abundances) of starless cores (e.g., see *Keto et al.*, 2004; *Lee et al.*, 2004b).

Surveys of starless cores have revealed many candidates with profiles suggestive of inward motions. For example, *Lee et al.* (1999), using CS (2–1) as an optically thick tracer and N_2H^+ (1–0) as an optically thin counterpart in single-pointing observations, found 17 of 220 optically selected "starless" cores with asymmetrically blue profiles. Subsequent modeling of these profiles suggested inward velocities of 0.04-0.1 km s^{-1}, i.e., subsonic. (The cores here are generally isolated and not found in turbulent molecular clouds.) *Lee et al.* (2004a) also observed 94 cores in the higher excitation CS (3–2) and DCO^+ (2–1) lines, finding 18 strong inward motion candidates. The average inward velocity of 10 cores derived from CS (3–2) was found to be slightly larger than the average velocity derived from CS (2–1), i.e., 0.07 km s^{-1} vs. 0.04 km s^{-1} respectively, suggesting more dense, inner gas moves faster than less dense, outer gas in these cores, though the statistical sample was small. Indeed, CS, being depleted in the central and denser regions of the cores (see Section 4), only traces the external (radii $\geq$ 7000 AU) envelope of the "chemically old" cores, so that the extended infall may reflect the (gravity driven) motion of the material surrounding these cores.

The nature of the inward motions observed in starless cores can be probed in detail through multi-line analyses of individual objects. For example, the isolated core in L1544 was found by *Tafalla et al.* (1998; see also *Williams et al.*, 1999) to have CS and H_2CO line profiles suggesting inward motions over a 0.2 pc extent. This scale is inconsistent with that expected from thermal "inside-out" collapse of a singular isothermal sphere since a central protostar of easily detectable luminosity would have likely formed in the time required for such a collapse wave to have propagated so far. (A CS/N_2H^+ mapping survey of 53 cores by *Lee et al.*, 2001 also found 19 with infall that was very extended.) In addition, the inward velocities determined via two-layer modeling were up to $\sim$0.1 km s^{-1}.

Although inward velocities derived from observations are larger than expected from some models of ambipolar diffusion, *Ciolek and Basu* (2000; CB00) argued that such motions could indeed result from magnetically retarded contraction through a background magnetic field of relatively low strength, e.g., $\sim$10 μG, and tailored a specific ambipolar diffusion model for the L1544 core. Multiple lines of N_2H^+ and N_2D^+ observed from L1544 by *Caselli et al.* (2002a) indeed showed some consistency with features of this model, including the velocity gradient observed across the minor axis and a slight broadening of line width and double-peaked line profiles at the core centre (possibly due to central depletion, but see *Myers*, 2005). Indeed, the ionization fraction of the L1544 core found by *Caselli et al.* (2002b) suggests its AD/FF timescale ratio $\approx$ 1 (see Section 4.3). The observed lines at central locations were wider than predicted from CB00, however, suggesting possible modifications such as turbulence and, in particular, an initial quasi-static layer contraction due to Alfvénic turbulence dissipation (e.g., *Myers and Zweibel*, 2001). Still more recent data have revealed further deviations from the CB00 model, however. For example, *van der Tak et al.* (2005) found evidence in double-peaked H_2D^+ 1_{10}–1_{11} line emission from the L1544 core for velocities (and densities) that are higher in its innermost regions than predicted by the CB00 model. (The CB00 model could fit N_2H^+ and $H^{13}CO^+$ data of the core but they sampled larger radii than H_2D^+.) Such velocities could occur if the central region of the L1544 core, where thermal pressure dominates, was smaller than predicted by CB00 model, or if collapse in these regions has become slightly more dynamic (but still subsonic).

Other isolated cores have shown inward velocities similar to those seen in L1544. For example, *Tafalla et al.* (2004) found evidence in N_2H^+ (1–0) line emission toward the L1498 and L1517B cores for relatively high velocity gas (i.e., $\sim$0.1 km s^{-1} offset from systemic velocities) that was coincident with regions of relatively high CS abundance. Such material may have been accreted onto the core only recently, suggesting a more stochastic growth of cores over time. In addition, *Williams et al.* (2006), comparing N_2H^+ 1–0 of the L694-2 and L1544 cores, found similar inward velocity increases with smaller projected radii, although the L694-2 core has a shallower gradient but a similar central value to that of the L1544 core (see Figure 4).

Not all starless cores show kinematic behaviour similar to L1544, however. For example, *Lada et al.* (2003) found both blue- and red-skewed profiles of CS (2–1) across the B68 core grouped in patterns reminiscent of a low-order acoustic oscillation mode. Since the B68 core may be more in structural equilibrium than the L1544 core (e.g., see *Alves et al.*, 2001), simultaneous inward and outward velocities of $\sim$0.1 km s^{-1} magnitude in the B68 core may not have to do with core contraction and expansion. Instead, such oscillations may have been excited by external influences, e.g., recent passage of a shock from expansion of the Loop I superbubble.

Ambipolar diffusion models like that of CB00 may not be required to explain inward motions within starless cores. For example, *Myers* (2005) has recently proposed that the pressure-free, gravitational collapse of non-singular, centrally concentrated gas configurations alone is sufficient to explain observed velocity features of starless cores; i.e., no magnetic retardation is required.

5.2 Turbulent Motions

Pressure support against gravity within starless cores is provided by both thermal and turbulent motions of the gas, in addition to what magnetic field pressure can impart to neutral species through ions. Observationally, widths of lines from undepleted molecules in starless cores can be used to probe the relative influence of thermal and nonthermal (turbulent) motions, and thus pressures in such cores, provided gas temperatures can be well determined (and magnetic field strengths; see chapter by *Ward-Thompson et al.*) Early NH_3 observations showed that low-mass dense cores have typically subsonic levels of gas turbulence (*Myers*, 1983). More recently, *Goodman et al.* (1998; see also *Barranco and Goodman*, 1998) found, in the cases they examined, that the width of the NH_3 lines within $\sim$0.1 pc of the core center does not follow the line width-size relations seen on large scales (e.g., $\Delta V \propto R^{0.5}$; see *Larson*, 1981), suggesting that starless cores may constitute localized islands of "coherence." *Goodman et al.* further speculated that this reduction of turbulent motions may be the result of dense cores at 0.1 pc providing a threshold for turbulent dissipation, e.g., through lower ion-neutral coupling from reduced internal ionization at high density and extinction.

Regions of quiescent line width in other starless cores were analyzed by *Caselli et al.* (2002c), who found a lack of general correlation between the N_2H^+ (1–0) line width and the core impact parameter in a sample of 26 cores, in agreement with earlier results. Furthermore, *Tafalla et al.* (2004; see also *Tafalla et al.*, 2002) found a close to constant dependence between the NH_3 or N_2H^+ line widths and impact parameter in the L1498 and L1517B cores. This breakdown of the line width-size relation has been replicated in recent numerical MHD models of dense cores, described elsewhere in this volume; e.g., see chapter by *Ballesteros-Paredes et al.* Large numbers of the "cores" produced in these models, although even resembling BES in density configuration, have larger internal velocities than the subsonic cores seen in Taurus. For example, *Klessen et al.* (2005) found only $<$23% of their model cores were subsonic. Comparisons between observed internal velocities of cores in other clouds and those predicted by turbulent models would be very interesting. Regions of quiescence within clustered cores have also been noted by *Williams and Myers* (2000) and *Di Francesco et al.* (2004). (For further discussion of the evolution of turbulent motions in cores, see the following chapter by *Ward-Thompson et al.*)

6. CONCLUSIONS

This review described the numerous recent observations and resulting inferences about the nature of starless cores. These objects represent the state of molecular gas preceding gravitational collapse that defines the initial conditions of star formation. Recent observations, together with recent advances in theory and experimental chemistry, have shown that these objects reside at different points on evolutionary paths from ambient molecular material to centrally concentrated, slowly contracting configurations with significant molecular differentiation. Though significant observational strides have been made, sensitivity and resolution limits on past instrumentation have in turn limited our ability to probe their internal physical and chemical properties. Fortunately, new instruments such as the wide-field line and continuum focal-plane arrays on single-dish telescopes like the JCMT, LMT, and the IRAM 30 m, Nobeyama 45 m, and APEX Telescopes, and the new sensitive interferometers like the SMA, CARMA, and ALMA will be available soon. These will provide the means to characterize numerous cores to high degrees, moving our understanding of their internal physical and chemical properties from an anecdotal to a statistical regime.

Acknowledgments. We thank an anonymous referee whose comments improved this review. NJE and PCM acknowledge support for this work as part of the Spitzer Legacy Science Program, provided by NASA through contract 1224608 issued by JPL, California Institute of Technology, under NASA contract 1407. In addition, NJE acknowledges support from NASA OSS Grant NNG04GG24G and NSF Grant AST-0307250 to the University of Texas at Austin. PC acknowledges support from the MIUR grant "Dust and molecules in astrophysical environments." PCM also acknowledges the support of NASA OSS Grant NAG5-13050. YA acknowledges the support from the COE Program at Kobe University and Grant-in-Aid for Scientific Research (14740130, 16036205) of MEXT, Japan.

REFERENCES

Aikawa Y., Ohashi N., Inutsuka S., Herbst E., and Takakuwa S. (2001) *Astrophys. J., 552*, 639-653.

Aikawa Y., Ohashi N., and Herbst E. (2003) *Astrophys. J., 593*, 906-924.

Aikawa Y., Herbst E., Roberts H., and Caselli P. (2005) *Astrophys. J.*, 620, 330-346.

Allen L. E., Myers P. C., Di Francesco J., Mathieu R., Chen H., et al. (2002) *Astrophys. J., 566*, 993-1004.

Allen M. and Robinson G. W. (1977) *Astrophys. J., 212*, 396-415.

Alves J. F., Lada C. J., and Lada E. A. (2001) *Nature, 409*, 159-161.

André P., Ward-Thompson D. A., and Motte F. (1996) *Astron. Astrophys., 314*, 625-635.

André P., Motte F., and Bacmann A. (1999) *Astrophys. J., 513*, L57-L60.

André P., Ward-Thompson D. A., and Barsony M. (2000) In *Protostars and Planets IV* (V. Mannings et al., eds.), pp. 59-96. Univ. of Arizona, Tucson.

André P., Bouwman J., Belloche A., and Hennebelle P. (2003) In *Chemistry as a Diagnostic of Star Formation* (C. L. Curry and M. Fich, eds.), pp. 127-138. NRC Press, Ottawa.

Bacmann A., André P., Puget J.-L., Abergel A., Bontemps S., et al. (2000) *Astron. Astrophys., 361*, 555-580.

Bacmann A., Lefloch B., Ceccarelli C., Castets A., Steinacker J., et al. (2002) *Astron. Astrophys., 389*, L6-L10.

Bacmann A., Lefloch B., Ceccarelli C., Steinacker J., Castets A., et al. (2003) *Astrophys. J., 585*, L55-L58.
Ballesteros-Paredes J., Klessen R. S., and Vázquez-Semadeni E. (2003) *Astrophys. J., 592*, 188-202.
Barranco J. A. and Goodman A. A. (1998) *Astrophys. J., 504*, 207-222.
Beichman C. A., Myers P. C., Emerson J. P., Harris S., Mathieu R., et al. (1986) *Astrophys. J., 307*, 337-339.
Belloche A. and André P. (2004) *Astron. Astrophys., 419*, L35-L38.
Benson P. J. and Myers P. C. (1989) *Astrophys. J. Suppl., 71*, 89-108.
Benson P. J., Caselli P., and Myers P. C. (1998) *Astrophys. J., 506*, 743-757.
Bergin E. A. and Langer W. D. (1997) *Astrophys. J., 486*, 316-328.
Bergin E. A. and Snell R. L. (2002) *Astrophys. J., 581*, L105-L108.
Bergin E. A., Plume R., Williams J. P., and Myers P. C. (1999) *Astrophys. J., 512*, 724-739.
Bergin E. A., Ciardi D. R., Lada C. J., Alves J., and Lada E. A. (2001) *Astrophys. J., 557*, 209-225.
Bergin E. A., Alves J., Huard T., and Lada C. J. (2002) *Astrophys. J., 570*, L101-L104.
Bergin E. A., Melnick G. J., Gerakines P. A., Neufeld D. A., and Whittet D. C. B. (2005) *Astrophys. J., 627*, L33-L36.
Bisschop S. E., Fraser H. J., Öberg K. I., van Dishoeck E. F., and Schlemmer S. (2006) *Astron. Astrophys.*, in press.
Black J. H. (1994) In *ASP Conf. Ser. 58, The First Symposium on the Infrared Cirrus and Diffuse Interstellar Clouds* (R. M. Cutri and W. B. Latter, eds.), pp. 355-367. ASP, San Francisco.
Bonnor W. B. (1956) *Mon. Not. R. Astron. Soc., 116*, 351-359.
Brown P. D. and Millar T. J. (1989) *Mon. Not. R. Astron. Soc., 240*, 25-29.
Caselli P., Myers P. C., and Thaddeus P. (1995) *Astrophys. J., 455*, L77-L80.
Caselli P., Walmsley C. M., Terzieva R., and Herbst E. (1998) *Astrophys. J., 499*, 234-249.
Caselli P., Walmsley C. M., Tafalla M., Dore L., and Myers P. C. (1999) *Astrophys. J., 523*, L165-L169.
Caselli P., Walmsley C. M., Zucconi A., Tafalla M., Dore L., et al. (2002a) *Astrophys. J., 565*, 331-343.
Caselli P., Walmsley C. M., Zucconi A., Tafalla M., Dore L., et al. (2002b) *Astrophys. J., 565*, 344-358.
Caselli P., Benson P. J., Myers P. C., and Tafalla M. (2002c) *Astrophys. J., 572*, 238-263.
Caselli P., van der Tak F. F. S., Ceccarelli C., and Bacmann A. (2003) *Astron. Astrophys., 403*, L37-L41.
Chandrasekhar S. (1957) "An Introduction to the Study of Stellar Structure", (Dover: Chicago), p. 155
Chandrasekhar S. and Wares G. W. (1949) *Astrophys. J., 109*, 551-554.
Chiar J. E., Adamson A. J., Kerr T. H., and Whittet D. C. B. (1995) *Astrophys. J., 455*, 234-243.
Chini R., Reipurth B., Ward-Thompson D., Bally J., Nyman L.-Å., et al. (1997) *Astrophys. J., 474*, L135-L138.
Chini R., Kämpgen K., Reipurth B., Albrecht M., Kreysa E., et al. (2003) *Astron. Astrophys., 409*, 235-244.
Choi M., Evans N. J., II, Gregersen E. M., and Wang Y. (1995) *Astrophys. J., 448*, 742-747.
Ciolek G. E. and Basu S. (2000) *Astrophys. J., 529*, 925-931.
Ciolek G. E. and Mouschovias T. Ch. (1995) *Astrophys. J., 454*, 194-216.
Clemens D. P. and Barvainis R. (1988) *Astrophys. J. Suppl., 68*, 257-286.
Crapsi A., Caselli P., Walmsley C. M., Myers P. C., Tafalla M., et al. (2005) *Astrophys. J., 619*, 379-406.
Dalgarno A. and Lepp S. (1984) *Astrophys. J., 287*, L47-L50.
De Vries C. H. and Myers P. C. (2005) *Astrophys. J., 620*, 800-815.
Di Francesco J., Myers P. C., and André P. (2004) *Astrophys. J., 617*, 425-438.
Doty S. D., Everett S. E., Shirley Y. L., Evans N. J., II, and Palotti M. L. (2005a) *Mon. Not. R. Astron. Soc., 359*, 228-236.
Doty S. D., Metzler R. A., and Palotti M. L. (2005b) *Mon. Not. R. Astron. Soc., 362*, 737-747.
Draine B. T. (1978) *Astrophys. J. Suppl., 36*, 595-619.
Draine B. T. and Lee H. M. (1984) *Astrophys. J., 285*, 89-108.
Ebert R. (1955) ZAp, 37, 217-232.
Egan M. P., Leung C. M., and Spagna G. F. (1988) *Comp. Phys. Comm., 48*, 271-292.
Ehrenfreund P. and Charnley S. B. (2000) *Ann. Rev. Astron. Astrophys., 38*, 427-483.
Emden R. (1907) *Gaskugeln*, Leipzig and Berlin, Table 14.
Enoch M. L., Young K. E., Glenn J., Evans N. J., II, Golwala S., et al. (2006) *Astrophys. J.*, in press.
Evans N. J., II, Rawlings J. M. C., Shirley Y. L., and Mundy L. G. (2001) *Astrophys. J., 557*, 193-208.
Evans N. J., II, Lee J.-E., Rawlings J. M. C., and Choi M. (2005) *Astrophys. J., 626*, 919-932.
Flower D. R., Pineau des Forêts G., and Walmsley C. M. (2005) *Astron. Astrophys., 436*, 933-943.
Galli D., Walmsley M., and Gonçalves J. (2002) *Astron. Astrophys., 394*, 275-284.
Geppert W. D., Thomas R., Semaniak J., Ehlerding A., Millar T. J., et al. (2004) *Astrophys. J., 609*, 459-464.
Gillett F. C. and Forrest W. J. (1973) *Astrophys. J., 179*, 483
Goldreich P. and Kwan J. (1974) *Astrophys. J., 189*, 441-453.
Goldsmith P. F. (2001) *Astrophys. J., 557*, 736-746.
Goodman A. A., Benson P. J., Fuller G. A., and Myers P. C. (1993) *Astrophys. J., 406*, 528-547.
Goodman A. A., Barranco J. A., Wilner D. J., and Heyer M. H. (1998) *Astrophys. J., 504*, 223-246.
Goodwin S. P., Ward-Thompson D., and Whitworth A. P. (2002) *Mon. Not. R. Astron. Soc., 330*, 769-771.
Gould R. J. and Salpeter E. E. (1963) *Astrophys. J., 138*, 393-407
Gregersen E. M. and Evans N. J. (2000) *Astrophys. J., 538*, 260-267.
Hara A., Tachihara K., Mizuno A., Onishi T., Kawamura A., et al. (1999) *Pub. Astron. Soc. Japan, 51*, 895-910.
Hartmann L. (2002) *Astrophys. J., 578*, 914-924.
Harvey D. W. A., Wilner D. J., Di Francesco J., Lee C. W., Myers P. C., et al. (2002) *Astron. J., 123*, 3325-3328.
Harvey D. W. A., Wilner D. J., Myers P. C., and Tafalla M. (2003) *Astrophys. J., 597*, 424-433.
Hatchell J., Richer J. S., Fuller G. A., Qualtrough C. J., Ladd E. F., et al. (2005) *Astron. Astrophys., 440*, 151-161.
Hennebelle P., Whitworth A. P., Cha S.-H., and Goodwin S. P. (2004) *Mon. Not. R. Astron. Soc., 348*, 687-701.
Herbst E. and Klemperer W. (1973) *Astrophys. J., 185*, 505-534.
Herbst E. and Leung C. M. (1989) *Astrophys. J. Suppl., 69*, 271-300.
Hirota T., Ikeda M., and Yamamoto S. (2001) *Astrophys. J., 547*, 814-828.
Hirota T., Ito T., and Yamamoto S. (2002) *Astrophys. J., 565*, 359-363.

Hirota T., Maezawa H., and Yamamoto S. (2004) *Astrophys. J., 617*, 399-405.
Hotzel S., Harju J., and Juvela M. (2002) *Astron. Astrophys., 395*, L5-L8.
Ivezić Ž., Nenkova M., and Elitzur M. (1999) *User Manual for DUSTY*, Univ. of Kentucky Internal Report.
Jessop N. E. and Ward-Thompson D. (2000) *Mon. Not. R. Astron. Soc., 311*, 63-74.
Jessop N. E. and Ward-Thompson D. (2001) *Mon. Not. R. Astron. Soc., 323*, 1025-1034.
Jijina J., Myers P. C., and Adams F. C. (1999) *Astrophys. J. Suppl., 125*, 161-236.
Johnstone D. and Bally J. (1999) *Astrophys. J., 510*, L49-L53.
Johnstone D., Wilson C. D., Moriarty-Schieven G., Joncas G., Smith G., et al. (2000) *Astrophys. J., 545*, 327-339.
Johnstone D., Fich M., Mitchell G. F., and Moriarty-Schieven G. (2001) *Astrophys. J., 559*, 307-317.
Johnstone D., Di Francesco J., and Kirk H. M. (2004) *Astrophys. J., 611*, L45-L48.
Jones C. E., Basu S., and Dubinski J. (2001) *Astrophys. J., 551*, 387-393.
Jørgensen J. K., Hogerheijde M. R., van Dishoeck E. F., Blake G. A., and Schöier F. L. (2004) *Astron. Astrophys., 413*, 993-1007.
Jørgensen J. K., Johnstone D., van Dishoeck E. F., and Doty S. D. (2006) *Astron. Astrophys.*, in press.
Jura M. (1974) *Astrophys. J., 191*, 375-379.
Kato S., Mizuno N., Asayama S., Mizuno A., Ogawa H., et al. (1999) *Pub. Astron. Soc. Japan, 51*, 883-893.
Kauffmann J., Bertoldi F., Evans N. J., II, et al. (2005) *Astron. Nach., 326*, 878-881.
Keto E., Rybicki G. B., Bergin E. A., and Plume R. (2004) *Astrophys. J., 613*, 355-373.
Kirk H. M., Johnstone D., and Di Francesco J. (2006), in press.
Kirk J. M., Ward-Thompson D., and André P. (2005) *Mon. Not. R. Astron. Soc., 360*, 1506-1526.
Klessen R. S., Ballesteros-Paredes J., Vázquez-Semadeni E., and Durán-Rojas C. (2005) *Astrophys. J.*, 620, 786-794.
Knez C., Boogert A. C. A., Pontoppidan K. M., Kessler-Silacci J. E., van Dishoeck E. F., et al. (2005) *Astrophys. J., 635*, L145-L148.
Kramer C., Alves J., Lada C. J., Lada E. A., Sievers A., et al. (1998) *Astron. Astrophys., 329*, L33-L36.
Kramer C., Richer J., Mookerjea B., Alves J., and Lada C. (2003), *Astron. Astrophys., 399*, 1073-1082.
Kuiper T. B. H., Langer W. D., and Velusamy T. (1996) *Astrophys. J., 468*, 761-773.
Lada C. J. and Lada E. A. (2003) *Ann. Rev. Astron. Astrophys., 41*, 57-115.
Lada C. J., Bergin E. A., Alves J. F., and Huard T. L. (2003) *Astrophys. J., 586*, 286-295.
Lai S.-P., Velusamy T., Langer W. D., and Kuiper T. B. H. (2003) *Astron. J., 126*, 311-318.
Larson R. B. (1981) *Mon. Not. R. Astron. Soc., 194*, 809-826.
Langer W. D. and Willacy K. (2001) *Astrophys. J., 557*, 714-726.
Langer W. D., van Dishoeck E. F., Bergin E. A., Blake G. A., Tielens A. G. G. M., et al. (2000) In *Protostars and Planets IV* (V. Mannings et al., eds.), pp. 29-57. Univ. of Arizona, Tucson.
Lee C. W. and Myers P. C. (1999) *Astrophys. J. Suppl., 123*, 233-250.
Lee C. W., Myers P. C., and Tafalla M. (1999) *Astrophys. J., 526*, 788-805.
Lee C. W., Myers P. C., and Tafalla M. (2001) *Astrophys. J. Suppl., 136*, 703-734.
Lee C. W., Myers P. C., and Plume R. (2004a) *Astrophys. J. Suppl., 153*, 523-543.
Lee J.-E., Evans N. J., II, Shirley Y. L., and Tatematsu K. (2003) *Astrophys. J., 583*, 789-808.
Lee J.-E., Bergin E. A., and Evans N. J., II (2004b) *Astrophys. J., 617*, 360-383.
Léger A. (1983) *Astron. Astrophys., 123*, 271-278.
Leung C. M. (1975) *Astrophys. J., 199*, 340-360.
Li Z.-Y. and Shu F. H. (1996) *Astrophys. J., 472*, 211-224.
Li Z.-Y., Shematovich V. I., Wiebe D. S., and Shustov B. M. (2002) *Astrophys. J., 569*, 792-802.
Lis D. C., Serabyn E., Keene J., Dowell C. D., Benford D. J., et al. (1998) *Astrophys. J., 509*, 299-308.
Lis D. C., Serabyn E., Zylka R., and Li Y. (2001) *Astrophys. J., 550*, 761-777.
Lombardi M. and Bertin G. (2001) *Astron. Astrophys., 375*, 1091-1099.
Lynds B. T. (1962) *Astrophys. J. Suppl., 7*, 1-52.
Mathis J. S., Mezger P. G., and Panagia N. (1983) *Astron. Astrophys., 128*, 212-229.
McCall B. J., Huneycutt A. J., Saykally R. J., Geballe T. R., Djuric N., et al. (2003) *Nature, 422*, 500-502.
Millar T. J., Bennett A., and Herbst E. (1989) *Astrophys. J., 340*, 906-920.
Mitchell G. F., Johnstone D., Moriarty-Schieven G., Fich M., and Tothill N. F. H. (2001) *Astrophys. J., 556*, 215-229.
Mizuno A., Hayakawa T., Tachihara K., Onishi T., Yonekura Y., et al. (1999) *Pub. Astron. Soc. Japan, 51*, 859-870.
Motte F., André P., and Neri R. (1998) *Astron. Astrophys., 336*, 150-172.
Motte F., André P., Ward-Thompson D., and Bontemps S. (2001) *Astron. Astrophys., 372*, L41-L44.
Murphy D. C. and Myers P. C. (2003) *Astrophys. J., 591*, 1034-1048.
Myers P. C. (1983) *Astrophys. J., 270*, 105-118.
Myers P. C. (2005) *Astrophys. J., 623*, 280-290.
Myers P. C. and Benson P. J. (1983) *Astrophys. J., 266*, 309-320.
Myers P. C. and Zweibel E. (2001) *Bull. Am. Astron. Soc., 33*, 915.
Myers P. C., Linke R. A., and Benson P. J. (1983) *Astrophys. J., 264*, 517-537.
Myers P. C., Fuller G. A., Goodman A. A., and Benson P. J. (1991) *Astrophys. J., 376*, 561-572.
Myers P. C., Mardones D., Tafalla M., Williams J. P., and Wilner D. J. (1996) *Astrophys. J., 465*, L133-L136.
Narayanan G. and Walker C. K. (1998) *Astrophys. J., 508*, 780-790.
Nutter D. J., Ward-Thompson D., and André P. (2005) *Mon. Not. R. Astron. Soc., 357*, 975-982.
Obayashi A., Kun M., Sato F., Yonekura Y., and Fukui Y. (1998) *Astron. J., 115*, 274-285.
Öberg K. I., van Broekhuizen F., Fraser H. J., Bisschop S. E., van Dishoeck E. F., et al. (2005) *Astrophys. J., 621*, L33-L36.
Ohashi N., Lee S. W., Wilner D. J., and Hayashi M. (1999) *Astrophys. J., 518*, L41-L44.
Oliveira C. M., Hébrard G., Howk C. J., Kruk J. W., Chayer P., et al. (2003) *Astrophys. J., 587*, 235-255.
Onishi T., Kawamura A., Abe R., Yamaguchi N., Saito H., et al. (1999) *Pub. Astron. Soc. Japan, 51*, 871-881.
Onishi T., Mizuno A., Kawamura A., Ogawa H., and Fukui Y. (1998) *Astrophys. J., 502*, 296-314.

Onishi T., Mizuno A., Kawamura A., Tachihara K., and Fukui Y. (2002) *Astrophys. J., 575*, 950-973.
Ossenkopf V. and Henning T. (1994) *Astron. Astrophys., 291*, 943-959.
Padoan P. and Scalo J. (2005) *Astrophys. J., 624*, L97-L100.
Padoan P., Willacy K., Langer W. D., and Juvela M. (2004) *Astrophys. J., 614*, 203-210.
Pagani L., Lagache G., Bacmann A., Motte F., Cambrésy L., et al. (2003) *Astron. Astrophys., 406*, L59-L62.
Pagani L., Bacmann A., Motte F., Cambrésy L., Fich M., et al. (2004) *Astron. Astrophys., 417*, 605-613.
Pagani L., Pardo J.-R., Apponi A. J., Bacmann A., and Cabrit S. (2005) *Astron. Astrophys., 429*, 181-192.
Pollack J. B., Hollenbach D., Beckwith S., Simonelli D. P., Roush T., et al. (1994) *Astrophys. J., 421*, 615-639.
Pontoppidan K. M., Dullemond C. P., van Dishoeck E. F., Blake G. A., Boogert A. C. A., Evans N, J., II, et al. (2005) *Astrophys. J., 622*, 463-481.
Redman M. P., Keto E., Rawlings J. M. C., and Williams D. A. (2004) *Mon. Not. R. Astron. Soc., 352*, 1365-1371.
Roberts H., Herbst E., and Millar T. J. (2003) *Astrophys. J., 591*, L41-L44.
Ruffle D. P., Hartquist T. W., Taylor S. D., and Williams D. A. (1997) *Mon. Not. R. Astron. Soc., 291*, 235-240.
Ruffle D. P., Hartquist T. W., Caselli P., and Williams D. A. (1999) *Mon. Not. R. Astron. Soc., 306*, 691-695.
Ryden B. S. (1996) *Astrophys. J., 471*, 822-831.
Sandell G. and Knee L. B. G. (2001) *Astrophys. J., 546*, L49-L52.
Schnee S. and Goodman A. A. (2005) *Astrophys. J., 624*, 254-266.
Shematovich V. I., Wiebe D. S., Shustov B. M., and Li Z.-Y. (2003) *Astrophys. J., 588*, 894-909.
Shirley Y. L., Evans N. J., II, Rawlings J. M. C., and Gregersen E. M. (2000) *Astrophys. J. Suppl., 131*, 249-271.
Shirley Y. L., Nordhaus M. K., Grcevich J. M., Evans N. J., II, Rawlings J. M. C., et al. (2005) *Astrophys. J., 632*, 982-1000.
Shu F. H. (1977) *Astrophys. J., 214*, 488-497.
Solomon P. M. and Werner M. W. (1971) *Astrophys. J., 165*, 41-49.
Stamatellos D. and Whitworth A. P. (2003) *Astron. Astrophys., 407*, 941-955.
Stamatellos D., Whitworth A. P., André P., and Ward-Thompson D. (2004) *Astron. Astrophys., 420*, 1009-1023.
Stanke T., Smith M. D., Gredel R., and Khanzadyan T. (2006) *Astron. Astrophys.*, in press.
Steinacker J., Bacmann A., Henning Th., Klessen R., and Stickel M. (2005) *Astron. Astrophys., 434*, 167-180.
Swift J., Welch W. J., and Di Francesco J. (2005a) *Astrophys. J., 620*, 823-834.
Tachihara K., Mizuno A., and Fukui Y. (2000) *Astrophys. J., 528*, 817-840.
Tachihara K., Onishi T., Mizuno A., and Fukui Y. (2002) *Astron. Astrophys., 385*, 909-920.
Tafalla M. and Santiago J. (2004) *Astron. Astrophys., 414*, L53-L56.
Tafalla M., Mardones D., Myers P. C., Caselli P., Bachiller R., et al. (1998) *Astrophys. J., 504*, 900-914.
Tafalla M., Myers P. C., Caselli P., Walmsley C. M., and Comito C. (2002) *Astrophys. J., 569*, 815-835.
Tafalla M., Myers P. C., Caselli P., and Walmsley C. M. (2004) *Astron. Astrophys., 416*, 191-212.
Tatematsu K., Umemoto T., Kandori R., and Sekimoto Y. (2004) *Astrophys. J., 606*, 333-340.
Tóth L. V., Haas M., Lemke D., Mattila K., and Onishi T. (2004) *Astron. Astrophys., 420*, 533-546.
van der Tak F. F. S. and van Dishoeck E. F. (2000) *Astron. Astrophys., 358*, L79-L82.
van der Tak F. F. S., Caselli P., and Ceccarelli C. (2005) *Astron. Astrophys., 439*, 195-203.
van Dishoeck E. F. (1988) In *Rate Coefficients in Astrochemistry* (T. L. Millar and D. A. Williams, eds.), p. 49-62. Kluwer, Dordrecht.
van Dishoeck E. F. (2004) *Ann. Rev. Astron. Astrophys., 42*, 119-167.
Vastel C., Phillips T. G., and Yoshida H. (2004) *Astrophys. J., 606*, L127-L130.
Walmsley C. M., Flower D. R., and Pineau des Forêts G. (2004) *Astron. Astrophys., 418*, 1035-1043.
Walsh A. J., Myers P. C., and Burton M. G. (2004) *Astrophys. J., 614*, 194-202.
Ward-Thompson D., Scott P. F., Hills R. E., and André P. (1994) *Mon. Not. R. Astron. Soc., 268*, 276-290.
Ward-Thompson D., Motte F., and André P. (1999) *Mon. Not. R. Astron. Soc., 305*, 143-150.
Ward-Thompson D., André P., and Kirk J. M. (2002) *Mon. Not. R. Astron. Soc., 329*, 257-276.
Watson W. D. and Salpeter E. E. (1972) *Astrophys. J., 174*, 321-340.
Williams J. P. and Myers P. C. (1999) *Astrophys. J., 518*, L37-L40.
Williams J. P., de Geus E. J., and Blitz L. (1994) *Astrophys. J., 428*, 693-712.
Williams J. P., Bergin E. A., Caselli P., Myers P. C., and Plume R. (1998) *Astrophys. J., 503*, 689-699.
Williams J. P., Myers P. C., Wilner D. J., and Di Francesco J. (1999) *Astrophys. J., 513*, L61-L64.
Williams J. P., Lee C. W., and Myers P. C. (2006) *Astrophys. J., 636*, 952-958.
Willacy K., Langer W. D., and Velusamy T. (1998) *Astrophys. J., 507*, L171-L175.
Wilson C. D., Avery L. W., Fich M., Johnstone D., Joncas G., et al. (1999) *Astrophys. J., 513*, L139-L142.
Womack M., Ziurys L. M., and Wyckoff S. (1992) *Astrophys. J., 387*, 417-429.
Yonekura Y., Mizuno N., Saito H., Mizuno A., Ogawa H., et al. (1999) *Pub. Astron. Soc. Japan, 51*, 911-918.
Young C. H., Jørgensen J. K., Shirley Y. L., Kauffmann J., Huard T., et al. (2004a) *Astrophys. J. Suppl., 154*, 396-401.
Young K. E., Lee J.-E., Evans N. J., Goldsmith P. F., and Doty S. D. (2004b) *Astrophys. J., 614*, 252-266.
Young K. E., Enoch M. L., Evans N. J., II, Glenn J., Sargent A. I., et al. (2006) *Astrophys. J.*, in press.
Yun J. L. and Clemens D. P. (1990) *Astrophys. J., 365*, L73-L76.
Yun J. L., Moreira M. C., Torrelles J. M., Afonso J. M., and Santos N. C. (1996) *Astron. J., 111*, 841-845.
Zhou S., Evans N. J., II, Kömpe C., and Walmsley C. M. (1993) *Astrophys. J., 404*, 232-246.
Zucconi A., Walmsley C. M., and Galli D. (2001) *Astron. Astrophys., 376*, 650-662.